

Journal of Materials Chemistry A

Accepted Manuscript



This is an *Accepted Manuscript*, which has been through the Royal Society of Chemistry peer review process and has been accepted for publication.

Accepted Manuscripts are published online shortly after acceptance, before technical editing, formatting and proof reading. Using this free service, authors can make their results available to the community, in citable form, before we publish the edited article. We will replace this *Accepted Manuscript* with the edited and formatted *Advance Article* as soon as it is available.

You can find more information about *Accepted Manuscripts* in the [Information for Authors](#).

Please note that technical editing may introduce minor changes to the text and/or graphics, which may alter content. The journal's standard [Terms & Conditions](#) and the [Ethical guidelines](#) still apply. In no event shall the Royal Society of Chemistry be held responsible for any errors or omissions in this *Accepted Manuscript* or any consequences arising from the use of any information it contains.

COMMUNICATION

Kinetic reconstruction of TiO₂ surfaces as visible-light-active crystalline phase with high photocatalytic performance

Cite this: DOI: 10.1039/x0xx00000x

Received 00th January 2012,
Accepted 00th January 2012

Peng Zheng,^{1,2} Ruipeng Hao,^{1,2} Jianghong Zhao,¹ Suping Jia,¹ Baoyue Cao,^{1,2}
Zhenping Zhu^{1*}

DOI: 10.1039/x0xx00000x

www.rsc.org/

The modulation of TiO₂ structure to meet efficient photocatalytic usage of solar light is still a challenging issue. Here we report that a simple bombardment of anatase TiO₂ nanocrystals by hot molecule can alter its phase transformation kinetics and leads to the reconstruction of the resulted rutile surfaces into a metastable TiO₂ crystalline structure. Moreover, the metastable surface crystalline phase is able to harvest the visible light up to 480 nm and exhibits a good property in photocurrent generation. Photocatalysis tests show that upon the irradiation of visible light (> 420 nm), the surface-reconstructed TiO₂ crystals display an excellent and stable photocatalytic activity for the hydrogen production from ethanol aqueous solution, with a hydrogen production rate of 302 μmol·g⁻¹·h⁻¹. This finding might bring on new approaches to kinetically tune the structure of TiO₂ or other semiconductor crystals for their property modulations.

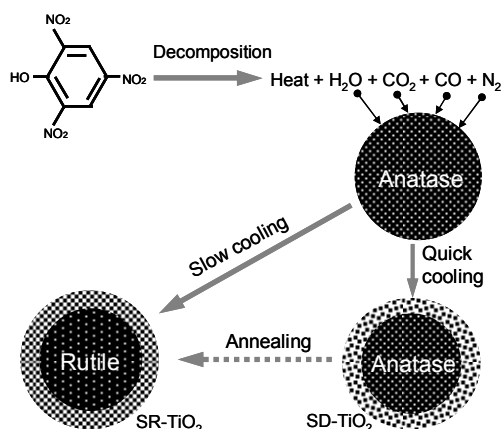
Since Fujishima and Honda found the photo-activity of TiO₂ in photoelectrochemical water splitting,¹ solar energy-driven hydrogen generation from water have attracted great attentions, especially in the today's context of energy shortage and environmental problems.²⁻⁴ To meet future practical applications, photocatalysts should exhibit multiple properties: well absorption of sunlight, high catalytic efficiency, high stability, and low cost. Although many photocatalysts have been proved to be active for hydrogen evolution from water,⁵⁻⁹ few of them can meet the multiple requirements. TiO₂ nanocrystals, especially anatase and rutile, have been widely accepted as promising photocatalytic materials due to their excellent photocatalytic properties, high stability, and rich resources. However, their wide band gaps (>3.0 eV) make them unable to harvest visible light, the major portion of solar spectrum. Much

effort has been focused on reducing their band gaps to extend their absorption spectrum. It has been well proved that the structural doping of TiO₂ with metal¹⁰ or non-metal¹¹⁻¹³ elements could effectively extend absorption spectrum, but the dopant-resulted defects often undesirably act as additional charge traps to induce the recombination of photo-generated electron-hole pairs and thus to decline photocatalytic activity heavily. As reported, the hydrogen production rates over the doped TiO₂ under visible light are normally at a level of tens μmol·g⁻¹·h⁻¹,¹³ about three orders of magnitude lower than that over pure TiO₂ nanocrystals under UV irradiation.

Recently, Mao et al.¹⁴ reported that the hydrogenation of TiO₂ can produce a color-black samples with disordered surface layers, which can increase solar absorption and support a hydrogen production from water under irradiation of > 400 nm light, at a rate of about 100 μmol·g⁻¹·h⁻¹. For efficient hydrogen generation over semiconductor catalysts, crystalline structure is desirable for quick charge transfer and the separation of electron-hole pairs¹⁵⁻¹⁷. Theoretical calculation predicted that new TiO₂ bulk phases with narrow band gaps might exist at extreme high pressure circumstances (48-60 Gpa),^{18,19} but they are impracticable for catalysis use due to their instabilities under normal conditions. Most recently, Iwasawa's and Batzill's groups^{20, 21} reported that new visible-light-responsive TiO₂ phases can be stabilized on the surfaces of normal TiO₂ bulk phases. Although they did not perform catalysis tests on their samples, their findings open a new strategy to modulate the light absorption window of TiO₂ photocatalysts by engineering their surfaces.

Herein, we report that upon a bombardment of anatase TiO₂ nanoparticles with high-pressure hot molecules produced from an explosive decomposition of trinitrophenol (TNP), the kinetics of the phase transformation from anatase to rutile can be simply modulated by controlling the subsequent cooling rate, by which the surfaces of rutile TiO₂ nanocrystals can be reconstructed as a new TiO₂ crystalline phase at a low cooling rate, as illustrated in Scheme 1.

The new surface phase can absorb visible light and exhibit good photocatalytic performance for hydrogen evolution from ethanol aqueous solution.



Scheme 1. Schematic illustration of the reconstruction of TiO_2 surfaces. Upon hot molecule bombardment, anatase TiO_2 surfaces can be controllably disordered (SD- TiO_2) or reconstructed as a new crystalline phase (SR- TiO_2).

The formation of the new surface phase of TiO_2 was observed when we attempted to disorder the surfaces of TiO_2 nanocrystals by a high-energy molecule bombardment for the preparation of TiO_2 photocatalysts with visible light activity, referring to Mao's strategy.¹⁴ As well known, the ultrafast decomposition (in a microsecond timescale) of explosive compounds such as trinitrophenol (TNP) produces huge heat and gaseous molecules (CO_2 , CO , H_2O , N_2) and thus can create unique high-temperature and high-pressure kinetic environments within sealed reactors. This feature was previously employed to induce decomposition of hydrocarbons for the syntheses of nano-sized diamonds²² and carbon nanotubes^{23,24} and to oxidize the surfaces of titanium nitride particles for the synthesis of nitrogen-doped TiO_2 photocatalysts with visible light activity.²⁵ In order to disorder TiO_2 nanocrystals on their surfaces, we used the high-pressure hot molecules generated from the explosive decomposition of TNP to bomb TiO_2 nanocrystals (commercial P25 nanoparticles) in a sealed stainless reactor (Supplementary Fig. S1). Experimentally, a mixture of the P25 nanoparticles and TNP was preloaded in the reactor, with desired mass and ratio. TNP explosive decomposition was induced by heating the reactor to about 310 °C in a tubular furnace and resulted in a high-temperature and high-pressure environment within the reactor, typically about 950 °C and 4.3 MPa. Just after TNP explosion, the reactor was immediately taken out the furnace to allow it cool quickly in air. By this way, the starting white P25 nanoparticles turned into black ones, with no obvious change in sizes (Supplementary Figs. S2a and S3a). When the reactor was allowed stay in the hot furnace for more than 10 minutes to slow down heat release rate, the TiO_2 nanoparticles would undergo an additional annealing process and turned into a sample with light-gray color (Supplementary Fig. S4a).

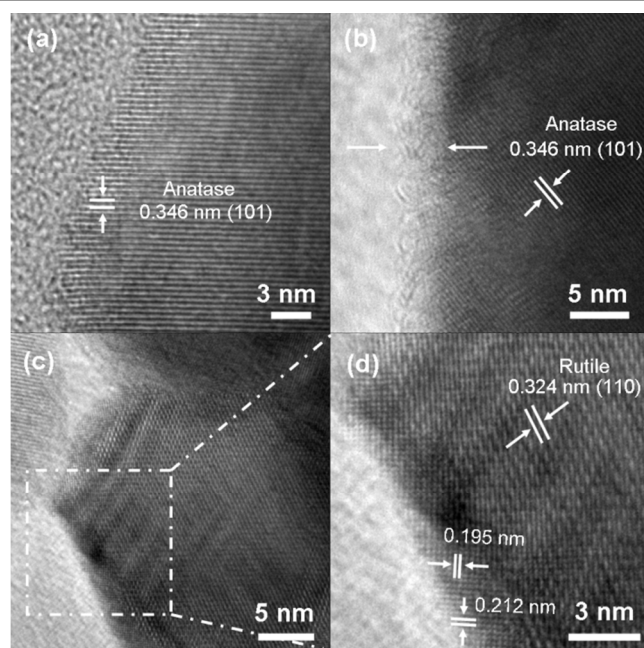


Figure 1. Typical HRTEM images of the obtained TiO_2 nanoparticles. (a) Original P25 nanoparticles. (b) The black TiO_2 nanoparticles obtained from a quick cooling behind the hot molecule bombardment. It shows an anatase core and a disordered surface. (c, d) The light-gray TiO_2 nanoparticles obtained from a slow cooling behind the hot molecule bombardment. It shows a rutile core and a surface with new crystalline structure.

As analyzed by high-resolution transmission electron microscopy (HRTEM), the starting P25 nanoparticles mainly display an anatase crystalline structure (Fig. 1a, Supplementary Fig. S2b-d), in consistent with the previous analyses.²⁶ Particularly, their surfaces are also highly ordered and have space lattices consecutively integrating with the bulk ones. Differently, in the black sample, majority of the TiO_2 nanoparticles exhibit disordered shells, while the bulk cores have a crystalline structure of anatase (Fig. 1b, Supplementary Figs. S3b-d). This observation indicates that the bombardment by the high-pressure hot gases makes TiO_2 nanoparticles lose their crystalline surfaces and form disordered layers, which might be associated with the black nature of the sample, similar to the situation reported by Mao et al.¹⁴ More interestingly, in the light-gray sample obtained from the additional annealing, although surface-disordered particles are also evident, many TiO_2 nanoparticles display a crystalline core-shell structure, with well-defined interfaces between the core crystals and shell crystals (Figs. 1c, 1d, Supplementary Figs. S4b-d). Based on careful observations on more than 50 particles, the cores always exhibit a rutile crystalline structure, with the distinctive lattice space of 0.324 nm belonging to the (110) facet of rutile TiO_2 . However, the crystalline shells visibly display two facets with plane distances of about 0.19 nm and 0.21 nm, which are perpendicular to each other and cannot be assigned to the crystal facets of any known TiO_2 bulk phases such as anatase, rutile, and brookite.^{27,28} This event suggests the formation of a new crystalline structure on the surfaces of rutile TiO_2 nanoparticles. For convenience in clear description, the black and light-gray TiO_2 samples are hereafter defined as surface-disordered TiO_2 (SD- TiO_2) and surface-reconstructed TiO_2 (SR- TiO_2), respectively.

We tried to analyze the SR-TiO₂ by X-ray diffraction (XRD) to understand the detailed crystalline structure of the new surface-reconstructed TiO₂ phase, but the effort failed because the surface phase is too small in size to give detectable diffraction signals. Both the SR-TiO₂ and SD-TiO₂ display diffraction patterns of a mixture of anatase and rutile phases (Supplementary Fig. S5), showing a partial bulk phase transformation from anatase to rutile. To further check the formation of the new crystalline surface phase of TiO₂, we have analyzed the samples by Raman spectroscopy, which is sensitive to the crystalline structures on material surfaces.²⁹ Compared with the starting P25, which displays a characteristic Raman scattering spectrum of anatase TiO₂ crystals³⁰, the SD-TiO₂ shows two additional weak and broad bands at about 442.6 and 617.1 cm⁻¹ (Fig. 2a), which reflects the presence of the amorphous surfaces.^{14,29} Differently, the SR-TiO₂ exhibits two new strong scattering bands near 247.7 and 435.8 cm⁻¹, which cannot be assigned to the bands of the known TiO₂ crystals anatase, rutile and brookite³⁰⁻³² and suggest the existence of new long-range ordered structure. This information, agreeing with the HRTEM observations, gives an additional evidence for the reconstruction of TiO₂ surfaces into a new crystalline phase.

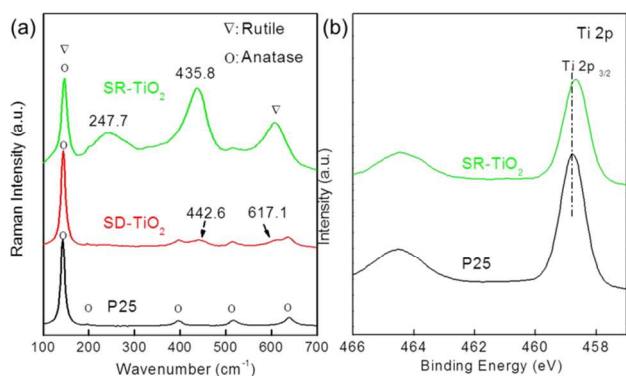


Figure 2. Surface structural characteristics of the modified TiO₂ nanoparticles. (a) Raman spectra of P25, SD-TiO₂ and SR-TiO₂. The strong scattering bands of the SR-TiO₂ at 247.7 and 435.8 cm⁻¹ suggest the existence of new surface crystalline phase. (b) Ti2p XPS spectra of P25 and SR-TiO₂.

As an effective surface analysis technique, X-ray photoelectron spectroscopy (XPS) can identify the electron state of the surface elements.³³ The Ti2p XPS spectrum of the SR-TiO₂ (Fig. 2b) exhibits a Ti2p_{3/2} signal at 458.65 eV, close to that of the original P25 (458.75 eV), suggesting a dominant structure of quadrivalent TiO₂. The slightly low binding energy might imply a partial production of low valence Ti species.³⁴ This is confirmed by electron paramagnetic resonance (EPR) analysis of the SR-TiO₂ (Supplementary Fig. S6), which displays a resonance signal at $g = 1.997$, revealing the existence of paramagnetic Ti³⁺ species.³⁵ Note that the original P25 shows no EPR signal, agreeing with the previous reports.³⁶

About the formation of the new surface crystalline phase, it is likely associated with the anatase-to-rutile phase transformation process and the unique kinetic environments created by the explosive decomposition of TNP. Combining the HRTEM observations with the XRD analyses (Supplementary Fig. S5), it is certain that upon the hot molecule bombardment of the anatase nanoparticles containing in original P25 there is a significant bulk

phase transformation from anatase to rutile, similar to the well-known heating-induced phase transformation.¹⁵ The new surface crystalline phase could be viewed as a metastable intermediate state formed kinetically during the anatase-to-rutile phase transformation. This conjecture is also supported by the inspections that the new surface phase was observed on the surfaces of rutile crystals rather than anatase crystals (Figs. 1c, 1d; Supplementary Figs. S4b-d) and that upon additional heating of the SR-TiO₂ at 750 °C in a tubular furnace, the new surface phase disappear and transforms into rutile phase. In addition, behind the superfast exothermal decomposition of TNP, the continuous heat diffusion through reactor wall that produces a dynamic cooling profile within reactor would predictably exercise different influences on the phase transformation kinetics of the bulks and surfaces of TiO₂ nanoparticles. The disordered surfaces observed in the SD-TiO₂, which was obtained at a high rate of heat diffusion, can be viewed as a frozen transient state of the consequence of the surface molecule bombardment. The new surface crystalline phase is likely formed from a re-crystallization of the disordered surface, as illustrated in Scheme 1, because the condition towards the SR-TiO₂ is just simply modified with the slowed heat diffusion. The transformed rutile structure in the cores might help to stabilize the metastable surface phase, similar to the remark by Batzill et al.²¹

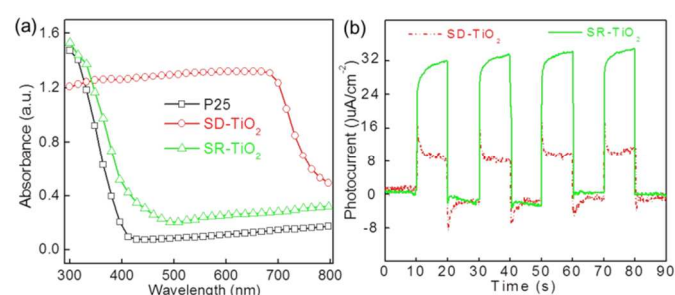


Figure 3. Visible light responses for the modified TiO₂ nanoparticles. (a) UV-visible absorption spectra of P25, SD-TiO₂ and SR-TiO₂. (b) The on/off amperometric I-t curves for the SD-TiO₂ and SR-TiO₂ photoanodes under the irradiation of > 420 nm light and zero bias, which show that SR-TiO₂ is more favorable for photocurrent generation.

Fig.3a presents the UV/vis absorption spectra of the SD-TiO₂ and SR-TiO₂, compared with that of the original P25. The SD-TiO₂ displays a strong platform absorption in quite wide range from 300 nm to 710 nm, which reflects its color-black feature, similar to the situation of the black TiO₂ obtained by Mao et al.¹⁴. The SR-TiO₂ has an absorption property more similar to that of the P25, with semiconductor-characteristic absorption edge, but its absorption edge obviously extends to visible light region, about 480 nm. This red shift in electron absorption can be assigned to the formation of the new surface crystalline phase because the accompanying bulk anatase-to-rutile phase transformation is unable to change the absorption spectrum so greatly.³⁷ The exactly phase composition of SR-TiO₂ and reason of its visible light absorption need further work.

We have also measured photocurrent generation on the SD-TiO₂ and SR-TiO₂ electrodes with an on-off transient response method,³⁸ as shown in Fig. 3b. Upon the irradiation of visible light (> 420 nm), photocurrent is readily generated on both SD-TiO₂ and SR-TiO₂ electrodes, with well reproducibility for numerous on/off cycles of illumination. Significantly, the photocurrent density on the SR-TiO₂

electrode is much higher than that on the SD-TiO₂ electrode, indicating that the former is more favorable for photoelectric transformation and/or for the separation of photo-excited electron-hole pairs.

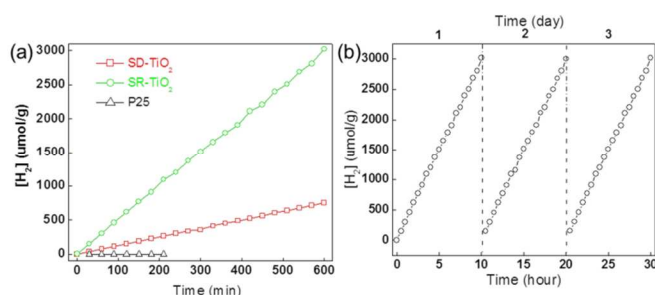


Figure 4. The photocatalytic behavior of the modified TiO₂ nanoparticles. (a) Photocatalytic H₂ evolution from ethanol aqueous solution over platinum-loaded P25, SD-TiO₂, and SR-TiO₂. Conditions: catalyst, 50 mg; Pt co-catalyst, 0.3 wt%; 20 vol% ethanol aqueous solution; light source, $\lambda > 420\text{nm}$ (300W Xe lamp with a cutoff filter). (b) A segmented cycling photocatalysis measurement over SR-TiO₂ for 30 h within 3 days, with the same conditions as those in (a).

The visible light activity and the photoelectric transformation property of the SD-TiO₂ and SR-TiO₂ make them potential photocatalysts with visible light response. As a demonstration, we have performed their photocatalytic abilities in the hydrogen production from an ethanol aqueous solution, as shown in Fig. 4a. Although the P25 sample is highly active for hydrogen generation under UV illumination,³⁹ it disables completely upon the irradiation of the light higher than 420 nm, while the modified SD-TiO₂ shows a considerable activity when a small amount of platinum co-catalyst is loaded on the surfaces, with a hydrogen evolution rate of 75 $\mu\text{mol g}^{-1}\text{h}^{-1}$. Interestingly, the SR-TiO₂ is more active under the same conditions, leading to a higher hydrogen evolution rate (302 $\mu\text{mol g}^{-1}\text{h}^{-1}$), more than four times of the SD-TiO₂ case. This event, agreeing with the situation of photocurrent measurement, is likely associated with the knowledge about photocatalysts: structural disorder would undesirably provide high-density trap for electron/hole recombination, while crystalline structure would facilitate the charge transfer and reduce the electron/hole recombination.^{2,4,40-43} Fig. 4a also shows that hydrogen generates at a constant rate within 10 h reaction for both the SD-TiO₂ and SR-TiO₂. Further sectional tests for the SR-TiO₂ illustrate a less loss after a segmented cycling reaction for 30 h within 3 days (Fig. 4b), and the position of its characteristic raman peaks had no change (Fig.S7) indicating a considerable stability of the formed surface crystalline phase, at least under the employed reaction condition.

Conclusions

In summary, we find that a new TiO₂ crystalline structure with visible light response can be constructed on the surfaces of rutile TiO₂ nanocrystals during the bulk phase transformation from anatase to rutile nanocrystals. This new surface phase can be viewed as a metastable intermediate structure and is formed and stabilized on rutile surfaces under an unusual kinetic condition. Furthermore, upon the irradiation of visible light ($> 420\text{ nm}$), the new surface crystalline phase exhibits excellent performances in photoelectric transformation and photocatalytic activity for the hydrogen production from

ethanol aqueous solution. This finding provides a possibility of kinetically modulating the structures of TiO₂ crystals to improve their light absorption and photocatalytic properties. Further researches on finding new kinetic approaches to tune the structures (phase and band) and photocatalytic properties of TiO₂ or other oxide semiconductors are believed to be quite interesting.

ACKNOWLEDGMENT

The authors acknowledge financial supports from National Natural Science Foundation of China (No. 21173250) and Chinese Academy of Sciences, following Solar Energy Plan Project (No. KG CX2.EW.311).

Notes and references

¹State Key Laboratory of Coal Conversion, Institute of Coal Chemistry, Chinese Academy of Sciences, Taiyuan 030001, China

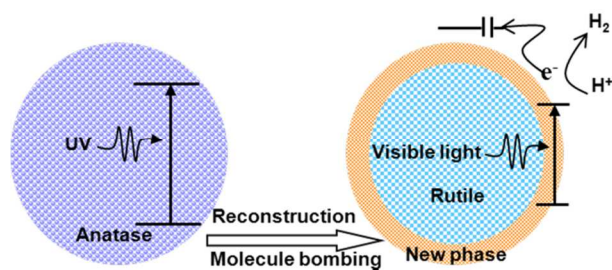
²University of Chinese Academy of Sciences, Beijing, 100049, China

† Experimental procedures and additional data. See DOI: 10.1039/c000000x/

- Fujishima, A.; Honda, K. *Nature* 1972, **238**, 37.
- Linsebigler, A. L.; Lu, G.; Yates, J. T. *Chem. Rev.* 1995, **95**, 735.
- Kudo, A.; Miseki, Y. *Chem. Soc. Rev.* 2009, **38**, 253.
- Kubacka, A.; Fernandez-Garcia, M.; Colon, G. *Chem. Rev.* 2012, **112**, 1555.
- Tong, H.; Ouyang, S. X.; Bi, Y. P.; Umezawa, N.; Oshikiri, M.; Ye, J. H. *Adv. Mater.* 2012, **24**, 229.
- Reece, S. Y.; Hamel, J. A.; Sung, K.; Jarvi, T. D.; Esswein, A. J.; Pijpers, J. J. H.; Nocera, D. G. *Science* 2011, **334**, 645.
- Xu, X.; Random, C.; Efstathiou, P.; Irvine, J. T. S. *Nat. Mater.* 2012, **11**, 595.
- Wang, X.; Maeda, K.; Thomas, A.; Takanabe, K.; Xin, G.; Carlsson, J. M.; Domen, K.; Antonietti, M. *Nat. Mater.* 2009, **8**, 76.
- Gueymard, C. A. *Solar Energy* 2004, **76**, 423.
- Choi, W.; Termin, A.; Hoffmann, M. R. *J. Phys. Chem.* 1994, **98**, 13669.
- Chen, X. B.; Burda, C. *J. Am. Chem. Soc.* 2008, **130**, 5018.
- Feng, N.; Wang, Q.; Zheng, A.; Zhang, Z.; Fan, J.; Liu, S.-B.; Amoureux, J.-P.; Deng, F. *J. Am. Chem. Soc.* 2013, **135**, 1607.
- Liu, G.; Pan, J.; Yin, L.; Irvine, J. T. S.; Li, F.; Tan, J.; Wormald, P.; Cheng, H.-M. *Adv. Funct. Mater.* 2012, **22**, 3233.
- Chen, X. B.; Liu, L.; Yu, P. Y.; Mao, S. S. *Science* 2011, **331**, 746.
- Zhang, J.; Xu, Q.; Feng, Z.; Li, M.; Li, C. *Angew. Chem. Int. Ed.* 2008, **47**, 1766.
- Tang, J.; Durrant, J. R.; Klug, D. R. *J. Am. Chem. Soc.* 2008, **130**, 13885.
- Ma, Y.; Xing, M.; Zhang, J.; Tian, B.; Chen, F. *Microporous Mesoporous Mat.* 2012, **156**, 145.
- Kim, D. Y.; de Almeida, J. S.; Koci, L.; Ahuja, R. *Appl. Phys. Lett.* 2007, **90**.
- Mattesini, M.; de Almeida, J. S.; Dubrovinsky, L.; Dubrovinskaia, N.; Johansson, B.; Ahuja, R. *Phys. Rev. B* 2004, **70**.
- Ariga, H.; Taniike, T.; Morikawa, H.; Tada, M.; Min, B. K.; Watanabe, K.; Matsumoto, Y.; Ikeda, S.; Saiki, K.; Iwasawa, Y. *J. Am. Chem. Soc.* 2009, **131**, 14670.
- Tao, J.; Luttrell, T.; Batzill, M. *Nat. Mater.* 2011, **3**, 296.
- Greiner, N. R.; Phillips, D. S.; Johnson, J. D.; Volk, F. *Nature* 1988, **333**, 440.
- Zhu, Z.; Lu, Y.; Qiao, D.; Bai, S.; Hu, T.; Li; Zheng, J. *J. Am. Chem. Soc.* 2005, **127**, 15698.
- Du, G.; Feng, S.; Zhao, J.; Song, C.; Bai, S.; Zhu, Z. *J. Am. Chem. Soc.* 2006, **128**, 15405.
- Zheng, P.; Zhao, J.; Zheng, J.; Ma, G.; Zhu, Z. *J. Mater. Chem.* 2012, **22**, 12116.

- 26 Zhang, J.; Zhang, Y.; Lei, Y.; Pan, C. *Catal. Sci. Technol.* 2011, **1**, 273.
- 27 Liao, Y.; Que, W.; Jia, Q.; He, Y.; Zhang, J.; Zhong, P. *J. Mater. Chem.* 2012, **22**, 7937.
- 28 Lin, H.; Li, L.; Zhao, M.; Huang, X.; Chen, X.; Li, G.; Yu, R. *J. Am. Chem. Soc.* 2012, **134**, 8328.
- 29 Yanagisawa, K.; Ovenstone, J. *J. Phys. Chem. B* 1999, **103**, 7781.
- 30 Ohsaka, T.; Izumi, F.; Fujiki, Y. *J. Raman Spectrosc.* 1978, **7**, 321.
- 31 Tompsett, G. A.; Bowmaker, G. A.; Cooney, R. P.; Metson, J. B.; Rodgers, K. A.; Seakins, J. M. *J. Raman Spectrosc.* 1995, **26**, 57.
- 32 Yang, G. D.; Jiang, Z.; Shi, H. H.; Xiao, T. C.; Yan, Z. F. *J. Mater. Chem.* 2010, **20**, 5301.
- 33 Tougaard, S.; Ignatiev, A. *Surf. Sci.* 1983, **129**, 355.
- 34 Saied, S. O.; Sullivan, J. L.; Choudhury, T.; Pearce, C. G. *Vacuum* 1988, **38**, 917.
- 35 Conesa, J. C.; Soria, J. *J. Phys. Chem.* 1982, **86**, 1392.
- 36 Xing, M.; Zhang, J.; Chen, F.; Tian, B. *Chem. Commun.* 2011, **47**, 4947.
- 37 Fujishima, A.; Zhang, X.; Tryk, D. A. *Surf. Sci. Rep.* 2008, **63**, 515.
- 38 Hu, S.; Xiang, C.; Haussener, S.; Berger, A. D.; Lewis, N. S. *Energy Environ. Sci.* 2013, **6**, 2984.
- 39 Gu, Q.; Long, J. L.; Zhou, Y. G.; Yuan, R. S.; Lin, H. X.; Wang, X. X. *J. Catal.* 2012, **289**, 88.
- 40 Beverly, K. C.; Sampaio, J. F.; Heath, J. R. *J. Phys. Chem. B* 2002, **106**, 2131.
- 41 Beverly, K. C.; Sample, J. L.; Sampaio, J. F.; Remacle, F.; Heath, J. R.; Levine, R. D. *Proc. Natl. Acad. Sci. U. S. A.* 2002, **99**, 6456.
- 42 Chandler, R. E.; Houtepen, A. J.; Nelson, J.; Vanmaekelbergh, D. *Phys. Rev. B* 2007, **75**.
- 43 Zhang, Q.; Uchaker, E.; Candelaria, S. L.; Cao, G. *Chem. Soc. Rev.* 2013, **42**, 3127.

Table of Contents artwork



Visible light responsive TiO₂ crystal forms on the surfaces of rutile TiO₂ nanocrystals during a kinetic phase transformation from anatase to rutile and exhibits excellent properties in photoelectric conversion and photocatalytic hydrogen production.